Astronomy & Astrophysics manuscript no. safari˙ns˙5˙2˙85 May 22, 2006
(DOI: will be inserted by hand later)

Oscillations of longitudinally density stratified coronal loops

H. Safari[1], S. Nasiri[1,2], and Y. Sobouti[1]

[1] Institute for Advanced Studies in Basic Sciences, Gava Zang, P.O. Box 45195-1159, Zanjan, Iran

[2] Department of Physics, Zanjan University, Zanjan, Iran

email: [hsafary, nasiri, sobouti]@iasbs.ac.ir

Received / Accepted

Abstract. The oscillations and wave propagation is studied in a cylindrical model of coronal loops that undergoes a longitudinal density stratification. Equations of motion are expressed by second order differential equations that are separable into radial and transverse components. The radial equation is solved in thin tube regime. The transverse equation is solved both by perturbation method, for small density scale heights, and numerically, otherwise.

Key words. Sun: corona — Sun: magnetic fields — Sun: Oscillations

1. Introduction

Since the earliest identification of the kink oscillations in coronal loops, reported by Aschwanden et al. (1999) and Nakariakov et al. (1999), a considerable amount of data has been analyzed by Aschwanden et al. (2002), Schrijver et al. (2002), and Wang & Solanki (2004) using the high resolution observations of TRACE, SoHO, Yohkoh, etc. See Aschwanden et al. (2004) and Nakariakov & Verwichte (2005) for an extended review.

The analysis of the oscillations of nine coronal loops by Verwichte et al. (2004) show shift in periods, phases, damping times, and distance-dependence of the amplitudes from those of the simple theoretical models of coronal loops (radially and longitudinally unstratified, cylindrical geometries with constant cross sections, constant magnetic fields along loop axes, constant gravitation, isothermal structures, no initial flows, etc).

There are numerous attempts to arrive at reasonably realistic models: Smith et al. (1997) and Van Doorsslare et al. (2004) have studied the effect of the curvature of the loop

Send offprint requests to: H. Safari

on the oscillations frequencies. Terra-Homem et al. (2003) give a detailed discussion of background flows in the loop. Nasiri (1992) simulates a variable cross section by assuming a long narrow wedge geometry. Ruderman (2003) removes the degeneracy inherent in loops of circular cross section by assuming an elliptical one. Díaz et al. (2004) introduce photospheric line-tying boundary conditions to emphasize the rate of leakage in damping of the oscillations. This is an extension of the infinite homogenous loops of Edwin & Roberts (1983). Beliën et al. (1996) find a gap in the continuous spectrum of Alfvén modes caused by longitudinal stratifications. Mendosa - Briceño et al. (2004) study the effect of the gravitational stratification. They find $10-20\%$ reduction in damping times of oscillations. Del Zanna et al. (2005) simulate 2.5-D compressible MHD oscillations in connection with solar atmospheric stratifications. They find a strong spreading in the initially localized pulses along the loop and correspondingly an efficient damping caused by the variable Alfvén velocity with height. Andries et al. (2005a, b) calculate damping rate of longitudinally stratified cylindrical loops and conclude that the ratio of the frequency of the first overtone to that of the fundamental mode is less than 2, the values for the unstratified loops. They use this ratio to estimate the density scale height in the solar atmosphere. Arregui et al. (2005) use the numerical code, POLLUX, to compute the effect of both radial and longitudinal stratification on the resonantly damped kink oscillations.

Here, we use analytical and numerical methods to study the effects of longitudinal density variation on loop oscillations. Density variations from interior to the exterior of the loop is stepwise. The functional form of the longitudinal stratification is, however, the same for both regions.

Equation of motions, boundary conditions, and the radial solutions are dealt with in Secs. 2& 3. Thin tube approximation is treated in Sec 4. Concluding remarks are given in Sec. 5.

2. Equations of motions

The linearized MHD equations for a zero-β plasma are

$$\frac{\partial \delta \mathbf{v}}{\partial t} = \frac{1}{4\pi\rho}\{(\nabla \times \delta\mathbf{B}) \times \mathbf{B} + (\nabla \times \mathbf{B}) \times \delta\mathbf{B}\}, \tag{1}$$

$$\frac{\partial \delta \mathbf{B}}{\partial t} = \nabla \times (\delta\mathbf{v} \times \mathbf{B}), \tag{2}$$

where $\delta\mathbf{v}$, $\delta\mathbf{B}$ and ρ are the Eulerian perturbations in the velocity, the magnetic field and the density, respectively. The simplifying assumptions are:

- Under coronal conditions gas pressure is negligible (zero- β).
- Tube geometry is a circular cylinder with cylindrical coordinates, (r,ϕ,z).
- There is a constant magnetic field along the z axis, $\mathbf{B} = B\hat{z}$.

– There is no initial steady flow in the loop or outside it.

– The equilibrium quantities are independent of ϕ.

– Time and ϕ- dependence for perturbed quantities is $exp[-i(\Omega t - m\phi)]$.

We are interested in the effects of density stratification with height $\rho_i(z)$ and $\rho_e(z)$ for the interior and exterior of the loop, respectively. With these assumptions, Eqs. (1) and (2) give the following coupled equations for δB_z and δv_r

$$\left(\frac{\Omega^2}{v_A^2}+\frac{\partial^2}{\partial z^2}-\frac{m^2}{r^2}\right)\frac{\delta B_z}{B}=\left(\frac{\Omega^2}{v_A^2}+\frac{\partial^2}{\partial z^2}\right)\frac{1}{r}\frac{\partial}{\partial r}(r\frac{\delta v_r}{i\Omega}), \tag{3}$$

$$\left(\frac{\Omega^2}{v_A^2}+\frac{\partial^2}{\partial z^2}\right)\frac{\delta v_r}{i\Omega}=-\frac{\partial}{\partial r}\frac{\delta B_z}{B}, \tag{4}$$

where $v_A(z)=B/\sqrt{4\pi\rho(z)}$ is the local Alfvén speed and is different for inside and outside of the loop. The term $\delta v_r/i\Omega$ appearing in Eqs. (4) and (3), is actually the lagrangian displacement vector in the loop. The remaining components of $\delta\mathbf{v}$ and $\delta\mathbf{B}$ are given by

$$\delta v_\phi = \frac{\Omega}{mB_z}r\delta B_z-\frac{1}{im}\frac{\partial}{\partial r}(r\delta v_r),\quad \delta v_z=0, \tag{5}$$

$$\delta B_r = -\frac{B_z}{i\Omega}\frac{\partial\delta v_r}{\partial z},\quad \delta B_\phi=-\frac{B_z}{i\Omega}\frac{\partial\delta v_\phi}{\partial z}. \tag{6}$$

See, e. g., Karami et al (2002) and Safari et al. (2005) for details. Let us also emphasize that the present form of Eq. (4) utilizes the fact that ρ and consequently v_A depend only on z. There is no radial stratification except for a step discontinuity at the surface of the tube.

Eliminating δv_r between Eqs. (4) and (3) gives

$$\left(\frac{1}{r}\frac{\partial}{\partial r}r\frac{\partial}{\partial r}+\frac{\partial^2}{\partial z^2}-\frac{m^2}{r^2}\right)\delta B_z+\frac{\Omega^2}{v_A^2}\delta B_z=0. \tag{7}$$

This is a wave equation for δB_z with the variable speed $v_A(z)$. It could be solved by the separation of variables. Let

$$\delta B_z=R(r)Z(z). \tag{8}$$

Equation (7) splits into

$$\left(\frac{d^2}{dr^2}+\frac{1}{r}\frac{d}{dr}-\frac{m^2}{r^2}\right)R(r)+k^2R(r)=0,\quad k^2=\frac{\Omega^2}{v_A^2|_{\epsilon=0}}-\kappa_z^2, \tag{9}$$

$$\left(\frac{d^2}{dz^2}-k^2\right)Z(z)+\frac{\Omega^2}{v_A^2}Z(z)=0, \tag{10}$$

where ϵ is in Eq. (14).

Each of Eqs. (9) and (10) are actually a pair for inside and outside of the tube. They are to be solved simultaneously for the values of R, Z, κ_z, and Ω.

2.1. Boundary conditions

1. To avoid shock waves at $r=a$, the lagrangian changes in pressure should be continuous. On account of the zero-β approximation and constancy of B, this reduces to the requirement of the continuity of δB_z. Thus

$$R^{\text{interior}}(a)=R^{\text{exterior}}(a). \tag{11}$$

2. On account of $\nabla \cdot \delta\mathbf{B} = 0$, δB_r should be continuous at $r = a$. This, gives (Karami et al 2002)

$$\frac{1}{k_i^2}\frac{dR^{\rm interior}(k_i r)}{dr}\bigg|_{r=a} = -\frac{1}{k_e^2}\frac{dR^{\rm exterior}(k_e r)}{dr}\bigg|_{r=a} \tag{12}$$

3. The footpoints, $z = 0$ & L, are expected to be nodes. This imposes the conditions

$$Z(z = 0 \ \& \ L) = 0. \tag{13}$$

Equation (11)- (13) give four boundary condition for the two second order differential Eqs. (9) & (10).

2.2. The density profile

We assume

$$\begin{aligned} \rho(\epsilon, z) &= \rho_i(\epsilon) f(\epsilon, z), \qquad r < a \\ &= \rho_e(\epsilon) f(\epsilon, z), \qquad r > a \end{aligned} \tag{14}$$

where $\rho_i(\epsilon)$ and $\rho_e(\epsilon)$ are the interior and exterior densities at the footpoints and a is the radius of the loop. $f(\epsilon, z)$ is envisaged to be a continuous function of z, with a minimum at $z = L/2$ and maxima $f(\epsilon, z = 0 \ \& \ L) = 1$. In the approximation of an isothermal loop in a constant gravity and bent into a semicircle with footpoints in the photosphere, one has (Andries et al. 2005b)

$$f(\epsilon, z) = exp(-\frac{\epsilon}{\pi}\sin\frac{\pi z}{L}), \tag{15}$$

where $\epsilon = L/H$ and H is the scale height. The density variations for inside an outside of the loop are governed by the same function $f(\epsilon, z)$. In the following we will consider loops of different scale heights but of the same total mass μ_i and μ_e. Thus,

$$\begin{aligned} &\mu_i = \rho_i(\epsilon)\int_0^L f(\epsilon, z)dz = \rho_i(\epsilon)(I_0(\epsilon) - \mathbf{L_0}(\epsilon)), \quad \text{independent from } \epsilon, \text{ or} \\ &\rho_i(\epsilon) = \mu_i/(I_0(\epsilon) - \mathbf{L_0}(\epsilon)) \end{aligned} \tag{16}$$

where I_0 and $\mathbf{L_0}$ are modified Bessel function of first kind and modified Struve function (see Gradsbteyn & Ryzbik, 2000). A similar relation holds for the outside of the loop.

3. Solutions of Eqs. (9) and (10)

Interior solutions of Eq. (9) are $J_m(|k_i|r)$ for $k_i^2 > 0$ or $I_m(|k_i|r)$ for $k_i^2 < 0$. Exterior solutions are $K_m(|k_e|r)$ for $k_e^2 < 0$ for evanescent waves or, $H_m(|k_e|r)$ for leaky decaying waves. Here we consider the evanescent category. Imposing the boundary conditions of Eqs. (11) and (12) give

$$\frac{1}{k_i}\frac{J_m'(|k_i|a)}{J_m(|k_i|a)} - \frac{1}{k_e}\frac{K_m'(|k_e|a)}{K_m(|k_e|a)} = 0, \tag{17}$$

where, $'$, indicates a derivative of a function with respect to its argument. The same relation holds for surface waves with $J_m(|k_i|r)$ replaced by $I_m(|k_i|r)$. For unstratified

thin and thick tubes Eq. (17) is analyzed by different authors, e. g., Edwin & Roberts (1983), Karami et al. (2002) and Safari et al. (2006). Here we study Eq. (17) for thin stratified loops by perturbational and numerical techniques.

4. Thin tube approximation

For $a/L \ll 1$ and $m \geq 1$ the dispersion relation of Eq. (17) gives $|k_i| \approx |k_e|$. From the definition of k^2, Eq. (9), one then obtains

$$\Omega = \kappa_z B[2\pi(\rho_i(0) + \rho_e(0))]^{-1/2}. \tag{18}$$

See also Edwin & Roberts (1978), Karami et al. (2002), Van Doorsselaere et al. (2004), Díaz et al. (2004). Substituting Eq. (18) in Eq. (10) yields

$$\begin{aligned} &\frac{d^2Z}{dz^2} + \frac{4\pi\Omega^2}{B^2}\frac{\rho_i(0)+\rho_e(0)}{2}F(\epsilon,z)Z(z) = 0, \\ &F(\epsilon,z) = \frac{2\rho_i(\epsilon,z)}{\rho_i(0)+\rho_e(0)} - \frac{\rho_i(0)-\rho_e(0)}{\rho_i(0)+\rho_e(0)}. \end{aligned} \tag{19}$$

This is an eigenvalue problem weighted by $F(\epsilon, z)$, from which one may write down the following integral expression for Ω^2

$$\Omega^2 = \frac{B^2}{2\pi(\rho_i(0)+\rho_e(0))}\frac{\int |dZ/dz|^2 dz}{\int F(\epsilon,z)|Z(z)|^2 dz}. \tag{20}$$

Some general relation of Ω^2 can be inferred from Eq. (20). In Fig. 1, $F(\epsilon, z)$ is plotted versus z for two values of ϵ. It has maxima at footpionts and a minimum at the apex. The larger the ϵ, the higher the maxima and the lower the apex. The larger ϵ, the higher the maxima and the lower the minimum become. For $\epsilon \geq 11.602$, $F(\epsilon, z)$ develops two roots z_1 and z_2, say. In the interval $z_1 - z_2$, $F(\epsilon, z)$ is negative. This reduces the integral in the denominator of Eq. (20) and cause an increase of Ω^2 with increasing ϵ. There is even the possibility of the integral, and thereby Ω^2, becoming negative. Our calculations shows that for $\rho_e/\rho_i = 0.1$ and for the fundamental this happens at $\epsilon = 30\pi$, such that

$$\begin{aligned} \Omega^2 > 0 \quad &\text{for } \epsilon < 30\pi \text{ and } |z_2 - z_1| < 0.95L \\ < 0 \quad &\text{for } \epsilon > 30\pi \text{ and } |z_2 - z_1| > 0.95L \end{aligned}$$

At $\epsilon = 30\pi$, Ω^2 has a vertical asymptote. This is

$$\begin{aligned} \Omega^2 \to +\infty \quad &\text{as for } \epsilon \to 30\pi \text{ from left} \\ \to -\infty \quad &\text{as for } 30\pi \leftarrow \epsilon \text{ from right.} \end{aligned}$$

This behavior is shown in Fig. 2.

Below Eq. (19) is solved for small density scale heights, by perturbation techniques, and for arbitrary scale heights, by numerical methods.

4.1. Perturbation method

The scale parameter is chosen as the perturbation parameter and all variables and equations are expanded in powers of ϵ. Thus,

$$\Omega = \Omega^{(0)} + \epsilon\Omega^{(1)} + \cdots, \tag{21}$$

$$Z(z) = Z^{(0)}(z) + \epsilon Z^{(1)}(z) + \cdots, \tag{22}$$

$$F(\epsilon, z) = 1 + \epsilon\frac{2\rho_i(0)}{\rho_i(0)+\rho_e(0)}\left(\frac{2}{\pi^2} - \frac{1}{\pi}sin\pi\frac{z}{L}\right) + \cdots, \tag{23}$$

Correspondingly Eq. (19) splits in it zeroth-order and first order components

$$\frac{d^2Z^{(0)}}{dz^2} + \frac{4\pi{\Omega^{(0)}}^2}{B^2}\frac{\rho_i(0)+\rho_e(0)}{2}Z^{(0)} = 0, \tag{24}$$

$$\frac{d^2Z^{(1)}}{dz^2} + \frac{4\pi{\Omega^{(0)}}^2}{B^2}\frac{\rho_i(0)+\rho_e(0)}{2}Z^{(1)} + \frac{8\pi\Omega^{(0)}\Omega^{(1)}}{B^2}\frac{\rho_i(0)+\rho_e(0)}{2}Z^{(0)} = -\frac{4\pi{\Omega^{(0)}}^2\rho_i(0)}{B^2}\left(\frac{2}{\pi^2} - \frac{1}{\pi}sin\pi\frac{z}{L}\right)Z^{(0)}, \tag{25}$$

Solutions of Eq. (24) for $Z^{(0)}$ and $\Omega^{(0)}$ with boundary conditions of Eq. (13) are

$$\Omega_l^{(0)} = \frac{l\pi}{L}B\sqrt{\frac{2}{4\pi(\rho_i(0)+\rho_e(0))}}, \quad l = 1, 2, 3, ..., \tag{26}$$

$$Z_l^{(0)}(z) = \sqrt{\frac{2}{L}}\sin\frac{l\pi}{L}z, \tag{27}$$

where l is the longitudinal mode number. The right side of Eq. (25) is a known perturbation term. Multiplying it by $Z^{(0)*}$, integrating and reducing it by Eq. (24) gives the first order correction to Ω

$$\Omega_l^{(1)} = \Omega_l^{(0)}\frac{\rho_i(0)}{\rho_i(0)+\rho_e(0)}(I_l - \frac{2}{\pi^2}) \tag{28}$$

where

$$I_l = \int_0^L Z_l^{(0)*}\frac{1}{\pi}sin\frac{\pi z}{L}Z_l^{(0)}dz = \frac{2}{\pi^2}\frac{4l^2}{4l^2-1}. \tag{29}$$

Equation (29) is in agreement with the result of Andries et al. (2005a) (see S_n in their Eqs. (3) and (4)). We note that a) $\Omega^{(1)}$ is positive, meaning that in loops of the same mass, the larger the stratification the larger the correction at to the frequencies of unstratified loop. b) for $l \gg 1$ the first order correction tend to zero. c) The ratio of the periods of the fundamental and the first overtone is

$$\frac{P_1}{P_2} = \frac{\Omega_2}{\Omega_1} = 2\frac{1+\epsilon\Omega_2^{(1)}/\Omega_2^{(0)}}{1+\epsilon\Omega_1^{(1)}/\Omega_1^{(0)}} = 2\frac{1+\epsilon\frac{\rho_i(0)}{\rho_i(0)+\rho_e(0)}\frac{2}{15\pi^2}}{1+\epsilon\frac{\rho_i(0)}{\rho_i(0)+\rho_e(0)}\frac{2}{3\pi^2}} < 2. \tag{30}$$

4.2. Numerical method

Using a numerical code based on shooting method Eq. (19) is solved for eigenvalues and eigenfunctions. In Fig. 3 the fundamental and the first overtone frequencies, Ω_1 & Ω_2,

respectively, and their ratio are plotted as functions of ϵ. As anticipated from Eq. (20) and the behavior of $F(\epsilon, z)$, both frequencies show monotonous increase with increasing ϵ. For small ϵ's Ω_1 has a steeper slope than Ω_2, but both approach each other as ϵ increases. The ratio P_1/P_2 begins at 2 for $\epsilon = 0$ and decreases to one at large ϵ's.

The longitudinal part of the eigenfield, $Z(z)$, is plotted in Figs. 4. For odd l values Figs. 4a & c as ϵ increases the middle antinode gradually flattens and eventually bifurcate into two humps with a dip in between. For both $l = 1$ & 3 this happens for $\epsilon \geq 3\pi$. The larger the epsilon the deeper the dip becomes. For both even and odd l's, the antinodes move towards the footpionts and away from each other with increasing ϵ.

5. CONCLUSIONS

We study the oscillations of vertically stratified model loops. In thin tube approximation the resulting eigenvalue problem is solved both by perturbational and numerical techniques.

- The ratio of periods of fundamental and first overtone modes, (2 for unstratified loops) decreases markedly and approaches 1 with increasing density scale parameter. This is in accord with the observational data of TRACE.
- The effect of density stratification is best understood by the behavior of $F(\epsilon, z)$. For small ϵ's it is all positive. But at large ϵ's it acquires negative values and there is the possibility of having $\Omega^2 < 0$, which means either dying or exponentially growing perturbations non-linear regimes.
- For $\rho_e/\rho_i = 0.1$, $\epsilon = 1.5$, and 2.85 the ratio P_1/P_2 are 1.841 and 1.679, respectively. These are in good agreement with the observational data of Verwichte et al. (2004), 1.81 ± 0.25 and 1.64 ± 0.23, respectively deduced from TRACE observations assuming the same density contrast and scale height parameter.
- The behavior of the eigenfunctions for different longitudinal wave numbers is completely different for unstratified and stratified loops. This is shown in Fig. 4 for $l = 1$, 2, and $l = 3$.

Acknowledgements. This work was supported by the Institute for Advanced Studies in Basic Sciences (IASBS), Zanjan. H. Safari wish to thank Prof. Robert Erdélyi for valuable consultations.

References

Andries, J., Goossens, M., Hollweg, J. V., Arregui, I., & Van Doorsselaere, T. 2005a, A&A, 430, 1109

Andries, J., Arregui, I., & Goossens, M. 2005b, ApJ, 24L, 57

Arregui, I., Van Doorsselaere, T., Andries, J., Goossens, M., & Kimpe, D. 2005, A& A, 441, 361

Aschwanden, M. J., De Pontieu, B., Schrijver, C. J., & Title, A. M. 2002, Sol. Phys., 206, 99

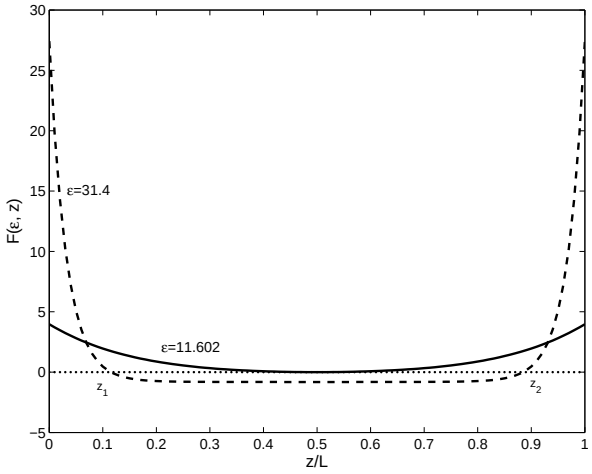

Fig. 1. $F(\epsilon, z)$ versus z/L. $\epsilon = 11.6$ (solid line), $\epsilon = 31.4$ (dashed line). For $\epsilon > 11.602$, $F(\epsilon, z)$ develops two roots, z_1 and z_2, say. Negative values of $F(\epsilon, z)$ in the internal $z_2 - z_1$.

Aschwanden, M. J., Fletcher, L., Schrijver, C. J., & Alexander, D. 1999, ApJ, 520, 880

Aschwanden, M.J., 2004, Physics of the Solar Corona- An Introduction, Praxis Publishing Ltd.: Chichester, UK, and Springer: New York, 842p.

Beliën, A. J. C., Poedts, S. & Goedbloed, J. P. 1996, Phys Rev Lett., 76(4), 567

Del Zanna, L., Schaekens, E. & Velli, M. 2005, A&A, 431, 1095

Díaz, A. J., Oliver, R., Ballester, J. L., & Roberts, B. 2004, A &A, 424, 1055

Edwin, P. M., & Roberts, B. 1983, Sol. Phys., 88, 179

Gradsbteyn, I. S., & Ryzbik, I. M., 2000, Academic Press, Table of Integrals, Series, and Products, 6^{th} Edition, 933

Karami, K., Nasiri, S. & Sobouti, Y. 2002, A&A, 396, 993

Mendoza-Briceño, César A., Erdélyi, R., & Sigalotti, Leonardo Di G., 2004, ApJ, 605, 493

Nakariakov, V. M., Ofman, L., Deluca, E. E., Roberts, B., & Davila, J. M. 1999, Science, 285, 862

Nakariakov, V. M., & Verwichte, E. 2005, LRSP, 2, 3

Nakariakov, V.M., & Ofman, L., 2001, A&A, 372, 53.

Nasiri, S. 1992, A&A, 261, 615

Ruderman, M. S. 2003, A&A 409, 287

Safari, H., Nasiri, S., Karami, K., & Sobouti, Y., 2006, A&A, 448, 375.

Schrijver, C. J., Aschwanden, M. J., & Title, A. 2002, Sol. Phys., 206, 69

Terra-Homem, M., Erdélyi, R.,& Ballai, I., 2003, Sol. Phys., 217, 199

Van Doorsselaere, T., Debosscher, A., Andries, J., & Poedts, S. 2004, A&A, 424, 1065

Verwichte, E., Nakariakov, V.M., Ofman, L., & DeLuca, E. E. 2004, Sol. Phys., 223, 77

Wang, T. J., & Solanki, S. K. 2004, A&A, 421, L33

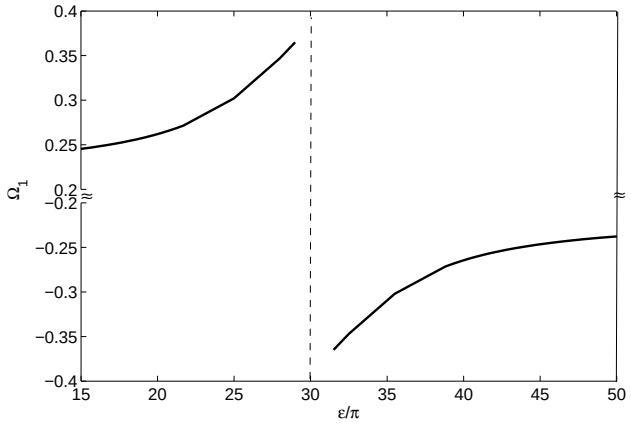

Fig. 2. The asymptotic behavior of the fundamental mode ($l = 1$) at $\epsilon = 30\pi$.

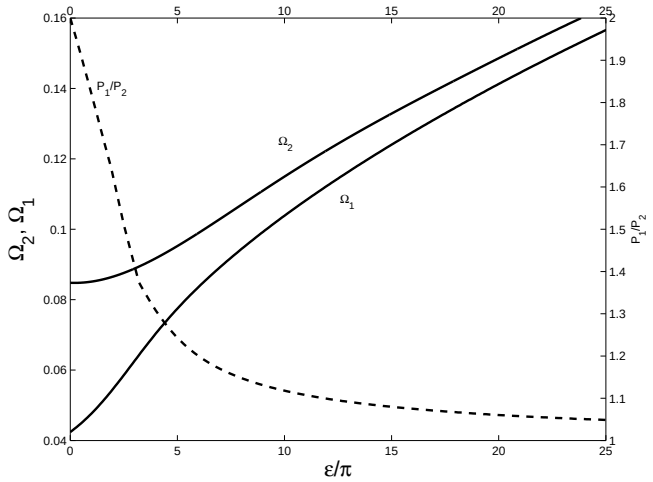

Fig. 3. The frequencies, Ω_1 and Ω_2, versus ϵ/π. The ratio of P_1/P_2, is versus ϵ/π. Auxiliary parameters are: the tube length $100a$, B = 100 G, and density contrast $\rho_e/\rho_i = 0.1$.

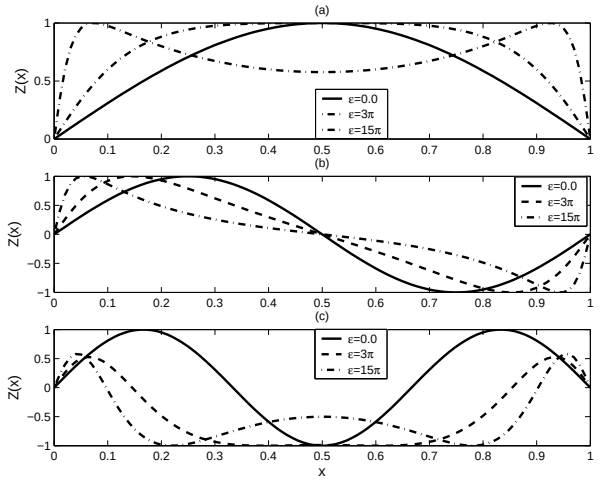

Fig. 4. a) The fundamental modes ($l = 1$), b) the first overtone modes ($l = 2$), and c) the second overtone modes ($l = 3$), for non- stratified, $\epsilon = 0$, and stratified, $\epsilon/\pi = 3,\ 15$, versus z.